ADVANCED ELECTRONIC MATERIALS
www.advelectronicmat.de

3D Printable and Biocompatible Iongels for Body Sensor Applications

Gisela C. Luque, Matías L. Picchio, Ana P. S. Martins, Antonio Dominguez-Alfaro, Nicolás Ramos, Isabel del Agua, Bastien Marchiori, David Mecerreyes, Roque J. Minari,* and Liliana C. Tomé**

Soft-ionic materials with biocompatibility and 3D printability are needed to develop next-generation devices to interface between electronic and biological signals. Herein, thermoreversible and biocompatible ionic liquid gels or iongels, which can be processed by direct ink writing are reported. The iongels are designed by taking advantage of polyvinyl alcohol/phenol interactions to gelify biocompatible cholinium carboxylate ionic liquids. The obtained iongels are stable, soft, and flexible materials (Young modulus between 14 and 70 kPa) with high ionic conductivity (1.8×10^{-2} S cm^{-1}). Interestingly, they presented thermoreversible properties with gel–sol transitions ranging from 85 and 110 °C, which allows the iongel processing via direct ink writing 3D printing by material extrusion at temperatures over its transition. These 3D printable iongels are integrated into a variety of body sensors applications, namely pressure sensors, motion sensors and electrodes for electrophysiological recordings. The iongels are used as pressure sensors with a sensitivity of 0.1 kPa^{-1}, ten times higher than that of others similar materials reported so far; showing its ability to detect human motion. Furthermore, the iongels showed excellent performance in electrodes for electrocardiography (ECG) recording, presenting good stability over time with electrocardiographic waves maintained their typical shape even after weeks.

1. Introduction

Artificial skin and wearable electronic devices are attracting remarkable attention because of the increase need of interaction with human body and long-term monitoring capabilities.[1] In particular, wearable devices that provide vital insights into the health of individuals in real-time have been developed in the last years. These devices require functional materials that are ultra-sensitive, comfortable, breathable, washable, flexible and robust.[2] In this scenario, next generation of bioelectronic based body sensors will need new soft-ionic systems for the interface between biology and electronics to improve the performance signals.

Ionic liquid gels, known as ionogels or iongels are a new generation of soft-ionic materials employed in several applications such as bioelectronics,[3] sensors,[4] energy,[5] and gas separation.[6] Particularly for bioelectronics, tailored iongels

Dr. G. C. Luque, Prof. R. J. Minari
Instituto de Desarrollo Tecnológico para la Industria Química (INTEC)
CONICET
Güemes 3450, Santa Fe 3000, Argentina
E-mail: rjminari@santafe-conicet.gov.ar
Dr. G. C. Luque, Prof. R. J. Minari
Facultad de Ingeniería Química
Universidad Nacional del Litoral
Santiago del Estero 2829, Santa Fe 3000, Argentina
The ORCID identification number(s) for the author(s) of this article can be found under https://doi.org/10.1002/aelm.202100178.
[+]Present address: LAQV-REQUIMTE, Chemistry Department, Faculdade de Ciências e Tecnologia, Universidade Nova de Lisboa, 2829-516 Caparica, Portugal

DOI: 10.1002/aelm.202100178

Dr. M. L. Picchio
Departamento de Química Orgánica
Facultad de Ciencias Químicas (Universidad Nacional de Córdoba)
IPQA–CONICET
Haya de la Torre y Medina Allende, Córdoba 5000, Argentina
A. P. S. Martins, Dr. A. Dominguez-Alfaro, N. Ramos,
Prof. D. Mecerreyes, Dr. L. C. Tomé[+]
POLYMAT
University of the Basque Country UPV/EHU
Joxe Mari Korta Center, Avda. Tolosa 72, Donostia-San Sebastian 20018, Spain
E-mail: david.mecerreyes@ehu.es; lilianasofi.carvalho@ehu.es
Dr. I. del Agua, Dr. B. Marchiori
Panaxium SAS
Aix-en-Provence 13100, France
Prof. D. Mecerreyes
Ikerbasque, Basque Foundation for Science
Bilbao 48013, Spain

need to present good mechanical properties, biocompatibility and adhesiveness. The key parameter to get a good register in body sensor applications is the adequate interface between the electrode and skin. For this reason, soft conducting coatings that decrease the impedance between the electrode and the skin have been developed in the last years.[7] Although hydrogels are currently used, the continuous evaporation of water makes difficult their long-term stability in open-air sensors. In this context, iongels are an excellent alternative since they show high ionic conductivity without suffering evaporation during the recording due to the negligible vapor pressure of the ionic liquid (IL). Therefore, several iongels have been developed for body sensor applications. In a pioneering work, Malliaras et al. reported electrophysiology recordings using an iongel onto gold and poly(3,4-ethylenedioxythiophene) doped with poly(styrene sulfonate) (PEDOT:PSS) electrodes. The iongel improved the performance of the electrodes and helped to maintain a low impedance over longer periods of time.[3] As a further improvement, Isik et al. developed cholininum-based iongels by photopolymerization of poly(choline lactate methacrylate) network within cholinium lactate IL, showing a stable recording of physiologic signals up to 72 h.[8] Later on, Bihar et al. employed inkjet printing to prepare electrodes from PEDOT:PSS on a commercial stretchable textile and the contact with the skin was improved by the addition of cholinium lactate-based iongel.[9] In what concerns the use of iongels as materials for strain and pressure sensors, Sun et al. reported an iongel prepared by photopolymerization of butyl acrylate (BA) in the IL 1-ethyl-3-methylimidazolium bis(trifluoromethy lsulfonylimide).[10] This strain sensor was able to detect human motions, human pulse and showed sensitivity in temperature sensing. On the other hand, Qin et al. reported a soft-ionic material based on gelatin and a deep eutectic solvent for ionic skin applications. The obtained gels exhibited a high stretchability and were capable to detect human motion.[11]

Additive manufacturing (AM) and 3D printing technologies are receiving tremendous attention as a versatile platform for the on-demand fabrication of objects and devices with excellent special control and functionality.[12,13] As recently highlighted by Nelson et al. "the future of additive manufacturing will depend on new polymeric materials that are specifically designed for these technologies".[14] In this context, ionic and/or electronic conducting polymers which are 3D printable have recently been actively searched for next-generation (bio)electronic devices. For this reason, there is an increasing interest in the development of soft ionic materials such as iongels and poly(ionic liquid)s that can be 3D printed.[15]

In this work, we report the first iongel which can be considered biocompatible and 3D printable. Although there have been examples of iongels for body sensor applications[16–23] and developed for 3D printing process,[24,25] to the best of our knowledge there are not reports about iongels that combine both. Therefore, biocompatible cholinium-based iongels were prepared by a simple method and formed by hydrogen bonding between poly(vinyl) alcohol (PVA) and plant-derived polyphenol compounds (PhCs). The mechanical and thermoreversible rheological properties, ionic conductivity and stability of the iongels were investigated. The 3D printing of the iongels was carried out by layer-by-layer direct ink writing. As final applications the iongels were tested in different body sensor devices such as ECG recording over time and as pressure sensor layers to detect human motion.

2. Results and Discussion

Thermoreversible supramolecular iongels were formed by a simple dissolution/cooling process as described in the experimental section. The mechanism for the supramolecular iongel formation is the hydrogen bonding dynamic crosslinking between PVA and different PhCs, namely gallic acid (GA), tanic acid (TA) and pyrogallol (PGA), in the presence of cholinium-based ILs combining acetate or lactate anions. The chemical structures of the iongel components and a schematic illustration of the supramolecular iongel formation are presented in **Figure 1**. It should be noted that all the iongel components are biocompatible,[26–29] and after their combination, iongels with 10% and 20% of polymer concentration were prepared. Figure S1 in the Supporting Information shows pictures of the prepared supramolecular cholinium-based materials. Iongles with different combination of PhC and ILs were obtained with 10% of polymer concentration. In the case of 20% of polymer concentration, it was just possible to obtain iongels with [Ch][Ac] and PGA, and [Ch][Lac] with GA and PGA, while in the other combinations the mixture did not dissolve.

The cholinium-based iongels were characterized by attenuated total reflection Fourier transform infrared (ATR-FTIR) spectroscopy to confirm their chemical structure and evaluate possible interactions in the supramolecular arrangement. As an example, the obtained ATR-FTIR spectra of the neat PVA, GA and [Ch][Lac], as well as the respective PVA-GA-[Ch][Lac] iongel are depicted in Figure S2 in the Supporting Information. The ATR-FTIR spectra obtained for PVA and GA were in agreement with those previously reported.[30,31] The presence of PVA and GA in the iongels can be confirmed by the peaks observed at 3014–3680 cm^{-1} attributed to the stretching vibration of OH groups, and the two bands at 2931 and 2853 cm^{-1} assigned to the asymmetrical and symmetrical stretching of CH groups, respectively. The C=O and C—OH stretching bands corresponding to GA can be seen at 1662 and 1309 cm^{-1}, respectively. The characteristic absorption bands of the [Ch][Lac] IL can also be found between 1300 and 1150 cm^{-1}, corresponding to the CN bond of the cholinium cation.[32] Nevertheless, no significant deviations in the abovementioned absorption bands were detected in the iongel spectra compared to those of the neat PVA, GA and [Ch][Lac] (Figure S2A in the Supporting Information). Similar results were obtained for the iongel systems containing TA and PGA as dynamic crosslinkers or [Ch][Ac] IL (Figure S2 in the Supporting Information). The high IL content is probably overlapping possible shifting of the absorption bands in the iongel formed by multiple hydrogen-bonding interactions. This is in agreement to what was previously observed for imidazolium-based iongels also obtained by supramolecular PVA/phenol interactions.[31]

The thermal properties of the iongels were analyzed by thermogravimetric analysis (TGA). The TGA results (Figure S3, Supporting Information) showed that the iongels presented good thermal stability, with maximum decomposition temperatures

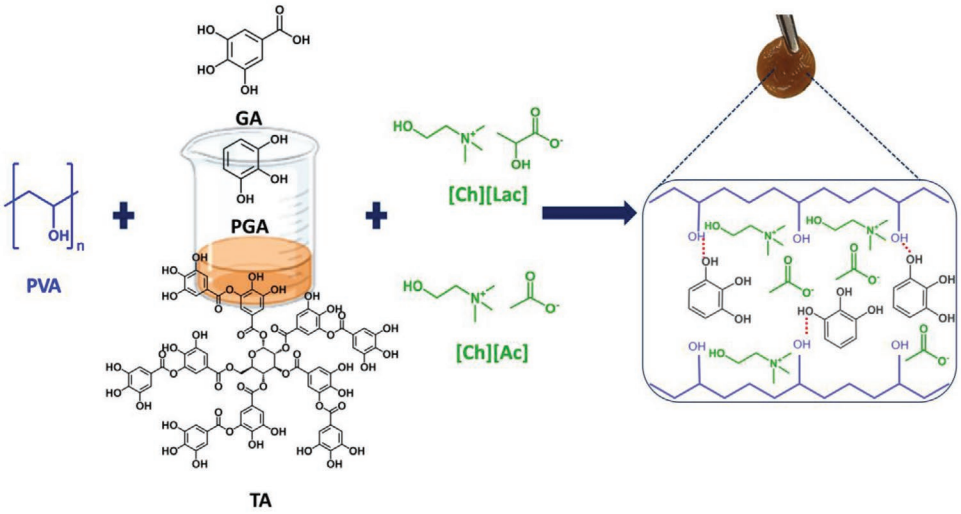

Figure 1. Schematic illustration of the supramolecular iongel formation, where PVA is combined with different PhCs (GA, PGA, TA) and two ILs (Cholinium Lactate and Acetate).

(T_{max}) between 225 and 240 °C in accordance with decomposition pattern of the polymer matrix. In addition, the TGA analysis revealed lower decomposition temperatures (at 50% of weight loss, $T_{50\%}$) for the iongels containing [Ch][Ac] than those of [Ch][Lac]. This is in agreement with the degradation profile of the neat ILs. The high thermal stability of the iongels is a valuable characteristic for 3D printing applications where materials can be subject to high temperatures over extrusion.

Ionic conductivity is one of the most characteristic properties of iongels and it is usually related with the good performance of different (bio)electronic devices.[33] Therefore, the ionic behavior of the supramolecular cholinium-based iongels was determined by impedance spectroscopy from 20 to 60 °C as shown in **Figure 2**A. The highest ionic conductivities were obtained for the iongel containing TA as dynamic crosslinker and [Ch][Lac] IL, with values ranging from 2.35×10^{-2} S cm^{-1} at 20 °C to 5.25×10^{-2} S cm^{-1} at 60 °C. Interestingly, these values were much higher than those reported by Isik et al. for [Ch][Lac]-based iongels, using a covalently crosslinked polymer host (ionic conductivity values at 60 °C range from 1×10^{-5} to 1×10^{-3} S cm^{-1}).[8] Others authors have also reported ionic conductivity values at 60°C of around 10^{-3} S cm^{-1} for iongels based on polycarbonates,[34] gel composed by a fluorocarbon elastomer and a fluorine-rich ionic liquid[35] and polyvinylchloride.[36] Therefore, these results suggest that the dynamic nature of our supramolecular iongels can probably facilitate the ions mobility inside the polymer network, boosting the ionic conductivity. Furthermore, the ionic conductivity of PVA-TA-[Ch][Lac] was evaluated during 70 h at 25 °C in order to study the ionic conductivity stability over time (Figure 2B). The PVA-TA-[Ch][Lac] iongel showed that conductivity values remained nearly constant and around 2×10^{-2} S cm^{-1} throughout the experiment. It should be mentioned that the weight of the PVA-TA-[Ch][Lac] iongel was recorded before each ionic conductivity measurement in order to identify possible gains or losses of water over time. Note that no significant changes were found in the iongel mass throughout the experiments. This represents a significant advantage of iongels when compared to hydrogels in body sensing applications. Hydrogels are susceptible to dehydration in the ambient environment and consequently, their ionic

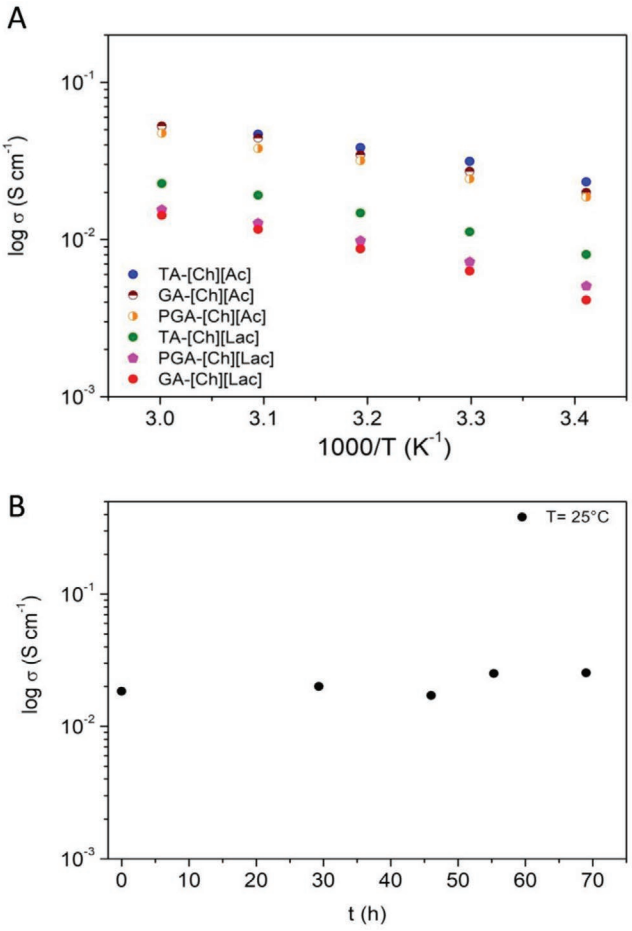

Figure 2. A) Variation of ionic conductivity of cholinium-based iongels with 10% polymer concentration. B) Variation of ionic conductivity with time of PVA-TA-[Ch][Lac].

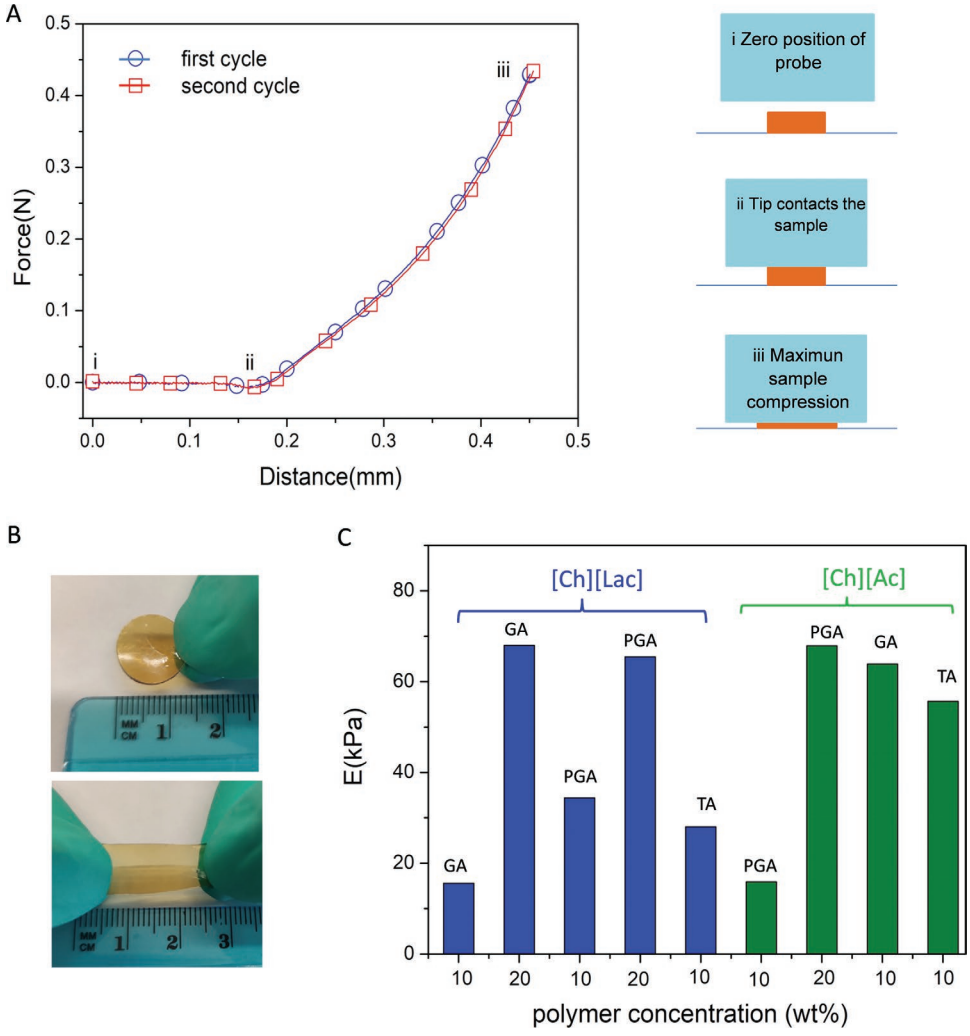

Figure 3. A) Force versus distance during two consecutive cycles of compression measured for the PVA-TA-[Ch][Lac] iongel (10% polymer concentration). B) Stretching of the PVA-TA-[Ch][Lac] iongel (10% polymer concentration). C) Compression modulus for the supramolecular cholinium-based iongels.

conductivity usually decrease due to water evaporation,[37,38] compromising the performance of the body sensor devices aimed to be implement during long time.

The mechanical and rheological properties of iongels are also important factors to take into account according to targeted applications. In particular, for bioelectronics, the interface materials are required to be soft, elastic and flexible. Following this line, the iongel were characterized under compression tests and the results are illustrated in **Figure 3**.

This iongel material, PVA-TA-[Ch][Lac], showed elastic behavior throughout the compression test and was able to resist deformation, recovering its initial shape after load removing. Two consecutive cycles of compression for PVA-TA-[Ch][Lac] iongel are depicted in Figure 3A, demonstrating the material's capability to recovery its original shape after each compression cycle. Namely, the distance at which the compression probe make contact with the sample (point ii in Figure 3A, which indicates the sample's height) was the same in both cycles. Remarkably, the PVA-TA-[Ch][Lac] iongel is very stretchable and elastic. As it can be seen from Figure 3B, no obvious cracks were observed when this iongel was extremely stretched close to its fracture strain, which is consistent with a good IL dispersion within a homogenous supramolecular network.

Compression curve (stress vs strain) for all of the samples are showed in Figure S4 (Supporting Information). Figure 3C shows the Young's modulus (E) calculated in the limit at low strain for the supramolecular cholinium-based iongels. As expected, the E modulus generally increases as the polymer concentration increased into the iongels, which is most likely attributed to the formation of additional intermolecular hydrogen bonding interactions. Nevertheless, contrary to what was previously reported regarding the formation of imidazolium-based iongels by supramolecular PVA/phenol interactions[31] the use of TA (the highest functional phenolic compound, Figure 1A) did not endow iongels with the highest E modulus. Concerning the influence of the different cholinium carboxylate ILs at 10 wt% polymer concentration, it can be observed from Figure 3C that the use of [Ch][Ac] resulted in higher E values for PGA and TA iongel systems, while lower E modulus were obtained for the GA-based iongels. On the other hand, at 20 wt% polymer

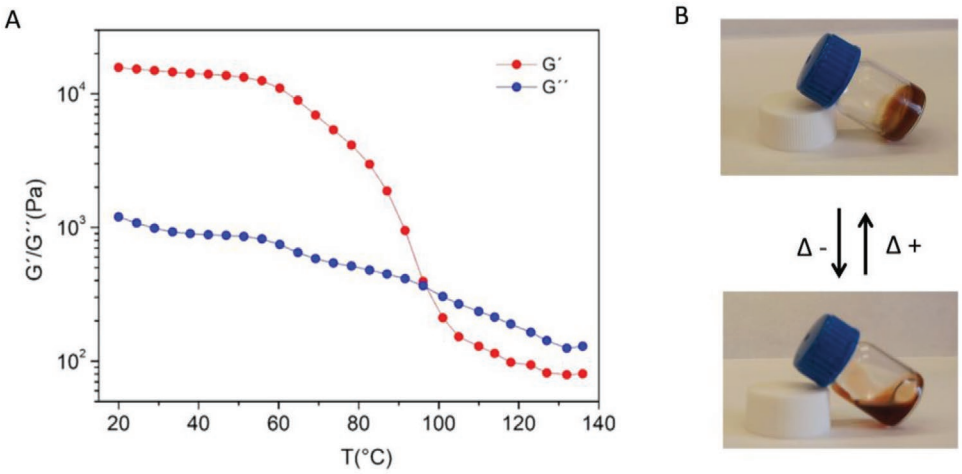

Figure 4. A) Thermomechanical behavior and B) Pictures of the reversible gel–sol phase transition of PVA-TA-[Ch][Lac] iongel.

concentration, no significant differences were observed on the *E* modulus for the different IL/PhC combinations tested.

In sum, and despite that the PVA-TA-[Ch][Lac] (10% wt) did not show the highest *E* modulus, this soft ionic material was selected amongst the different supramolecular cholinium-based iongels to continue our studies due to its high ionic conductivity and elasticity performance (Figures 2A and 3C).

The rheological properties of the supramolecular cholinium-based iongels were investigated by dynamic mechanical thermal analysis (DMTA). As a typical example, **Figure 4**A shows the viscoelastic behavior as a function of the temperature for the PVA-TA-[Ch][Lac] iongel with 10 wt% polymer concentration. In general, the supramolecular cholinium-based iongels displayed solid-like behaviors at temperatures below 85 °C, as the elastic modulus (G') is above the viscous modulus (G''). However, a transition from an elastic network to a viscoelastic liquid ($G'' > G'$) occurred when the temperature overpass the gel–sol phase transition temperature ($T_{gel\text{-}sol}$), defined as the temperature at which $G'' = G'$. $T_{gel\text{-}sol}$ was found to be between 85 and 110 °C for the supramolecular cholinium-based iongels prepared in this work (Table S2, Supporting Information). Contrary to our expectations, the $T_{gel\text{-}sol}$ of these materials was not affected by the type of PhC used, although an effect of using different IL was observed in Table S2 in the Supporting Information. For example, for a polymer concentration of 10%, lower $T_{gel\text{-}sol}$ (around 10 °C) were obtained for iongels with [Ch][Ac] in comparison to [Ch][Lac]. On the other hand, it become obvious that increasing the polymer content from 10 to 20 wt% led to higher $T_{gel\text{-}sol}$ of the iongels due to the higher number of hydrogen bonding interactions formed. It is worth noting that all the iongels displayed reversible gel–sol phase transitions (Figure 4B), which is a crucial requisite for their use as printable soft ionic materials in bioelectronics.

The prepared Iongels, which contain ILs with essentially zero vapor pressure, are not subject to liquid out flow, which affords significant advantages compared to hydrogels in terms of their ability to be processed using different methods. In particular, 3D printing is an enabling technology to fabricate physical objects, based on layers-by-layer material depositions from 3D models pre-designed by computer, for a wide range of applications ranging from tissue engineering to flexible electronics, sensors and many others.[39,40] In this work, considering that the supramolecular cholinium-based iongels have thermoreversible properties, we decide to explore the 3D printing of the PVA-TA-[Ch][Lac] iongel by extrusion, where the material has to flow through the nozzle and needs to undergo rapid regelation just after ejection in order to maintain high shape fidelity of the printed structure. A scheme illustrating the 3D printing process and patterns is presented in **Figure 5**A, while some pictures of the employed equipment are shown in Figure 5B. In this manner, the PVA-TA-[Ch][Lac] iongel was printed applying two material layers. Although printed materials displayed in this paper have planar patterns, this study will allow extending to the development of new 3-D-shaped devices.

As it can be seen in Figure 5C, the material printed on top of the substrate was able to resist the mechanical demands of deformation without showing obvious signals of damage or discontinuity. Overall, these results demonstrated that the supramolecular iongel proposed in this work are printable, soft and elastic materials, while the 3D printing process by material extrusion is a good alternative for the fabrication of sensors and electrodes according to the design requirements of each bioelectronic device. As a proof of concept of the capability of prepared iongels for bioelectronics device fabrication by 3D printing process, pressure sensor and two types of electrodes, kapton and textile, were successfully obtained (Figure S5 and Videos S1–S3, Supporting Information available in (https://drive.google.com/drive/folders/13HWVKiufA6wRzLbcmtKAtOJ8KxNUU8vx?usp=sharing)), though they were not tested for ECG recordings.

With the growing interest in human-electronics interaction, the development of devices exhibiting human skin-like sensory capabilities, such as mechanical force and temperature changes, is widely spreading.[41] For instance, pressure sensors are devices able to transduce mechanical changes into electrical signals and have been intensively investigated for electronic skin,[42,43] wearable electronics,[44,45] and soft robotics applications.[46] In view of the soft, stretchable and compressive properties, as well as high ionic conductivity and self-adhesiveness of the supramolecular cholinium-based iongels, a pressure sensor

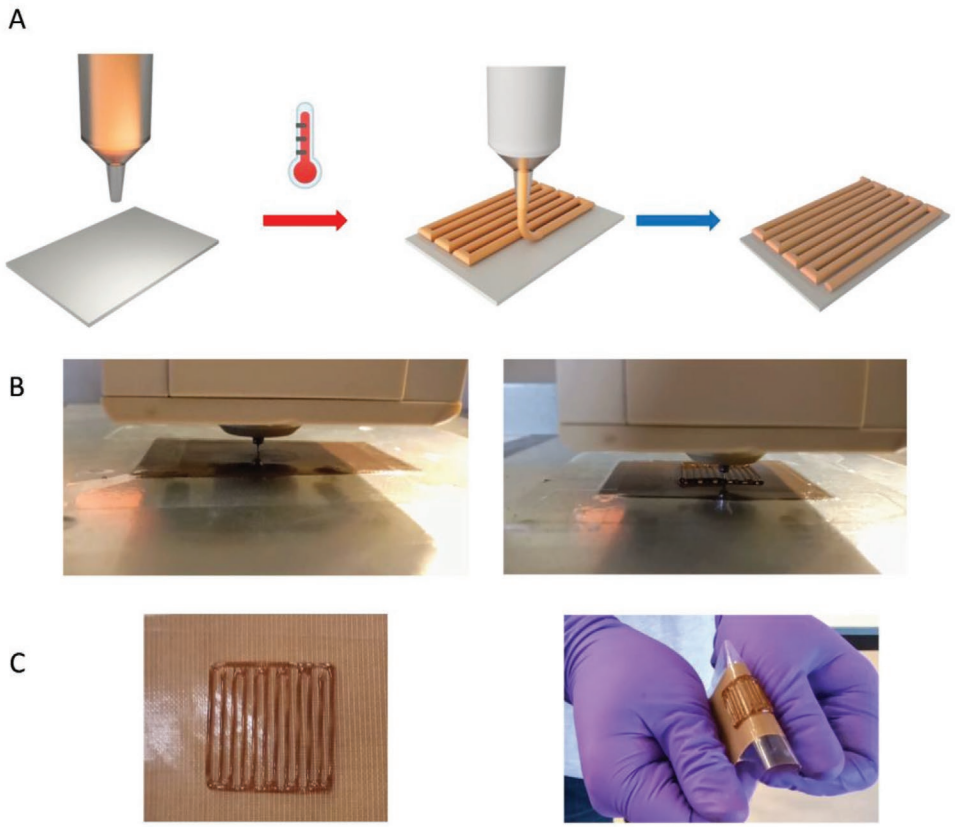

Figure 5. 3D printing process A) Scheme B,C) Pictures of the 3D printing patterns of PVA-TA-[Ch][Lac] supramolecular iongel at 10% polymer concentration.

was developed to demonstrate the pressure sensing ability of an ionic skin device containing the PVA-TA-[Ch][Lac] iongel.

The pressure sensor was assembled as described in the Experimental Section and as it is schematically illustrated in **Figure 6**A. Two iongel layers were fabricated by 3D printing from a previously synthesized PVA-TA-[Ch][Lac] iongel. Then, the pressure sensor has a sandwich type structure, where the two iongels layers are separated by an insulating plastic film with a thickness of around 20 µm. The performance of the pressure sensor was evaluated by measuring the capacitance values when different pressures were applied. As it can be seen from Figure 6B, the relative capacitance change (delta C/C_0) increased approximately linearly as pressure was applied from 1 to 10 kPa. With this information, the pressure sensitivity can be defined as the slope of the curve (Figure 6B).[47] In that sense, a higher slope values indicates a better sensor sensitivity, involving a higher relative capacitance change per pressure unit. In this context, our pressure sensor exhibited a good sensitive, being able to detect small changes in the applied pressure, with a sensitivity of 1 kPa^{-1} at low pressure values (<1 kPa, Figure S6A in the Supporting Information shows the evolution of the relative capacitance change in pressure range below 1 kPa) and 0.1 kPa^{-1} at high pressure values (between 1 and 10 kPa). These values of sensitivity are better than the ones reported in literature. Zhouyue et al. reported a gelatin-supported deep eutectic solvent gel with a sensibility of 0.01 kPa^{-1} below 2 kPa.[11] The same group also prepared a bioinspired mineral hydrogel with sensitivity as pressure sensor of 0.17 kPa^{-1}.[48] Xiong et al. presented a sandwich structure of ionic hydrogels and elastomer films for energy conversion and tactile sensing with a sensitivity value of 0.13 kPa^{-1}.[49]

Additionally, constructed pressure sensors were subjected to consecutive cycles of pressure (extended until 200 kPa). The obtained results are depicted in Figure S6B (Supporting Information) and demonstrate the reversibility of the pressure sensor incorporating the PVA-TA-[Ch][Lac] iongel. This also unveils that the sensor has the capacity to recover its initial dimensions and capacitance values. Due to supramolecular cholinium-based iongel materials are flexible and capable of being elastically deformed, their respective pressure sensors are able to conform readily to curved surfaces. Accordingly, we attached the PVA-TA-[Ch][Lac]-based pressure sensor onto the joint of an extended human finger, by stretching the sensor as the finger was bent. The relative capacitance change was measured as the finger was repeatedly bent and extended (Figure 6C). Notably, a relative capacitance change of 300% was obtained in each cycle. This experiment not only demonstrates the feasibility of the pressure sensor device to detect finger bending, but also suggests the great potential of our supramolecular cholinium-based iongels to detect other types of human motion in ionic skin applications.

The supramolecular cholinium-based iongels were also tested to assist electrodes in cutaneous electrophysiology. Selected iongels were incorporated onto Kapton and textile electrodes and then used as the electrolytic interface between the

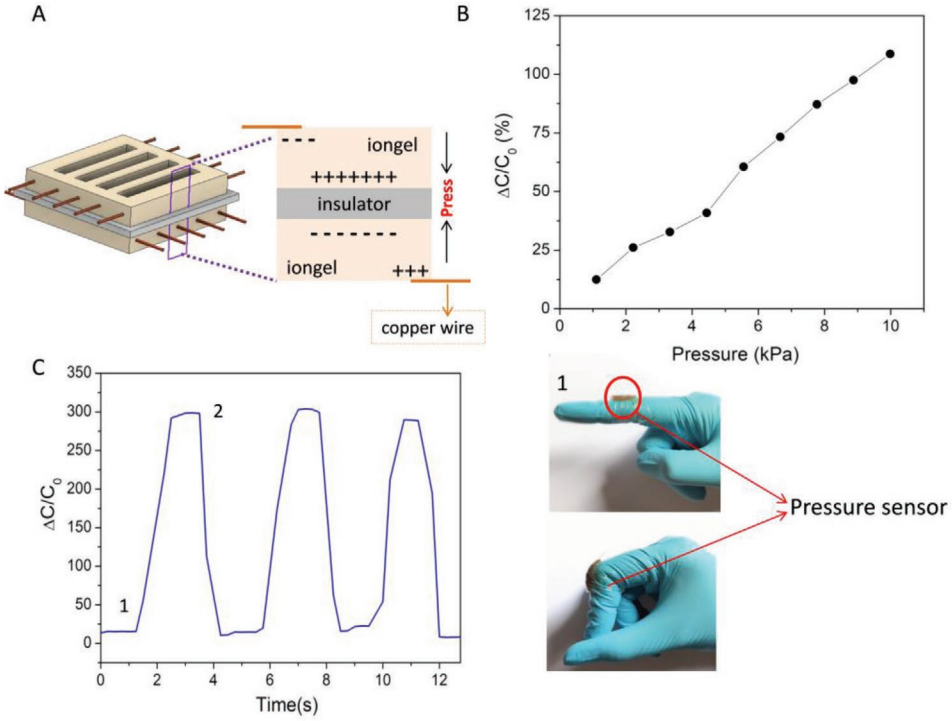

Figure 6. A) Schematic structure and operating principle of the pressure sensor device built with PVA-TA-[Ch][Lac] iongel at 10% polymer concentration. B) Relative capacitance change-pressure curve of the pressure sensor (C_0 = 680 nF). C) Pictures of the finger stretching the pressure sensor and relative capacitance change measured while the finger was cyclically bent and extended.

electrodes and the skin. The performance of these electrodes in cutaneous recordings was tested by measuring the ECG signals on a healthy volunteer (**Figure 7**A). The Kapton electrodes containing PVA-PGA-[Ch][Lac] and PVA-TA-[Ch][Lac] iongels displayed similar performance of ECG recordings compared to medical standard electrodes (Figure 7B).

In order to evaluate the long-term recording capability of the PVA-TA-[Ch][Lac] iongel, the response of this iongel assisted textile electrode in ECG measurements was regularly recorded for two weeks (Figure 7C,D). It should be mentioned that PEDOT:PSS textile electrodes are proven to be good candidates as wearable electrodes,[50,51] since they are stretchable and durable. Hence, the heart activity was recorded using a PVA-TA-[Ch][Lac] iongel assisted textile bracelet PEDOT:PSS electrode at the time of fabrication (t = 0) and after one day (t = 24 h), two days (t = 48 h), one week (t = 1 w), and 2 weeks (t = 2 w). From Figure 7C,D, it can be perceived that the bracelet electrode maintaining good quality EGC recordings during two weeks at normal environmental conditions. Actually, the ECG recordings did not show any significant degradation of the signal during this period of time, indicating that the integrity of the PVA-TA-[Ch][Lac] iongel is well-preserved even upon exposure to environmental and skin humidity. In sum, the supramolecular cholinium-based iongels are highly attractive options for long-term monitoring of electrophysiological activity since these soft ionic materials do not leak or dry out, maintaining their performance over time, and having the extra advantage of being all made from biocompatible components when compared to other iongel systems that have been investigated for this application.[3,8,51] In terms of performance, the ECG measurements in Figure 7 show amplitudes of the peaks between 400 and 500 μV, which is comparable with the reported performance of electrodes containing cholinium based Iongel of similar structure (400 μV).[8]

3. Conclusions

This work reports the preparation, characterization and applications of cholinium-based supramolecular iongels, which were obtained by a simple method employing polyphenols, PVA, and cholinium lactate and cholinium acetate as ionic liquids. These iongels are flexible, elastics with Young modulus between 14 and 70 kPa, and present high and stable ionic conductivity values ranging from 2.35×10^{-2} S cm^{-1} at 20 °C to 5.25×10^{-2} S cm^{-1} at 60 °C. In addition, the iongels showed thermoreversible sol-gel transition between 85 and 107 °C, allowing their use for 3D printing process as a tool to create electrodes (kapton and textile) and a pressure sensor. The fabricated pressure sensor was capable to detect human motion and showed a high sensitivity (0.1 kPa^{-1}) with an excellent reversibility. Furthermore, the proposed supramolecular cholinium-based iongels presented an excellent performance for long-lasting ECG recording, until 2 weeks, and the response was comparable to that of commercial medical electrodes. Altogether, these innovative supramolecular iongels will open up new avenues in the field of 3D-printable soft devices for bioelectronics, where a vast assortment of new materials could emerge from the combination of different polyphenols, biocompatible ionic liquids, and biodegradable polymer matrices.

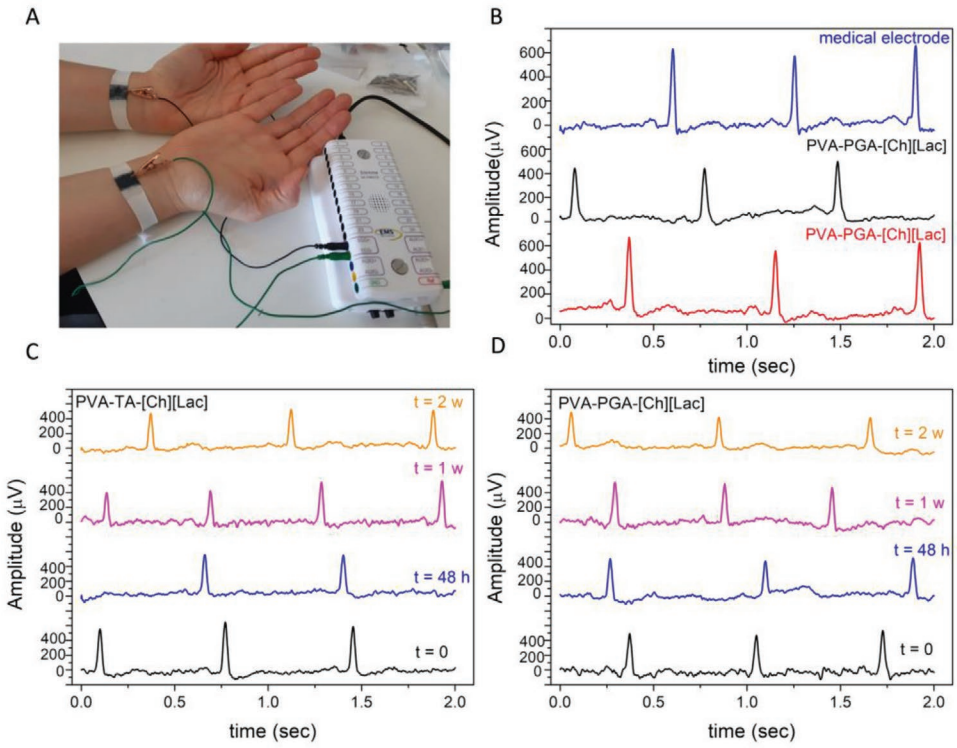

Figure 7. A) Picture of ECG performed. B) ECG performed with medical electrode, PVA-TA-[Ch][Lac] and PVA-PGA-[Ch][Lac] iongels- C,D) ECG performed with PVA-PGA-[Ch][Lac] and PVA-TA-[Ch][Lac] iongels over two weeks. The iongels polymer concentration was 10 wt% and the tested electrodes were produced by molding.

4. Experimental Section

Materials: Poly(vinyl alcohol) (PVA, Merck, degree of hydrolysis 99%, Mw 145 kDa), gallic acid (GA, Merck, ≥99.0%), pyrogallol (PGA, Carlo Erba, ACS reagent), tannic acid (TA, Biopack, ACS reagent), acetic acid (Sigma Aldrich), choline bicarbonate (Sigma Aldrich) and lactic acid (Sigma Aldrich) were used as received. Distilled-deionized water was used for all experiments. Poly(3,4-ethylenedioxythiophene): poly(styrene sulfonate) (PEDOT:PSS) (Clevios PH1000, Heraeous), ethylene glycol (EG) (Sigma Aldrich), 4-dodecylbenzenesulfonic acid (DBSA) (Sigma Aldrich) and divinyl sulfone (DVS) (Sigma Aldrich).

Synthesis of Cholinium Carboxylate Ionic Liquids: Cholinium acetate ([Ch][Ac]) and cholinium lactate ([Ch][Lac]) were synthesized by dropwise addition of the corresponding acid (1:1) to aqueous choline bicarbonate, following an established procedure.[28,52] The mixtures were stirred at room temperature for 12 h. The resulting products were washed several times with diethyl ether to remove unreacted acid. Excess of water and traces of the organic solvent were removed first by rotary evaporation, and then by stirring and heating under vacuum at moderate temperature (40–50 °C). The chemical structures and purities of the cholinium-based ILs were confirmed by ^{1}H- and ^{13}C-NMR.

Cholinium Acetate: ^{1}H NMR (400 MHz, D_2O): δ/ppm = 1.75 (s, 3H, CH_3COO); 3.04 (s, 9H, $N(CH_3)_3$); 3.35 (t, 2H, NCH_2CH_2OH); 3.90 (m, 2H, NCH_2CH_2OH). ^{13}C NMR (101 MHz, D_2O): δ/ppm = 23.23 (s, CH_3COO); 53.71 (t, $N(CH_3)_3$); 55.49 (s, NCH_2CH_2OH); 67.29 (t, NCH_2CH_2OH); 181.05 (s, $OOCCH(CH_3)OH$).

Cholinium Lactate: ^{1}H NMR (400 MHz, D_2O): δ/ppm = 1.17 (d, 3H, $OOCCH(CH_3)OH$); 3.07 (s, 9H, $N(CH_3)_3$); 3.38 (t, 2H, NCH_2CH_2OH); 3.92 (m, 2H, NCH_2CH_2OH); 3.97 (q, 1H, $OOCH(CH_3)OH$). ^{13}C NMR (101 MHz, D_2O): δ/ppm = 19.83 (s, $OOCCH(CH_3)OH$); 53.74 (t, $N(CH_3)_3$); 55.52 (s, NCH_2CH_2OH); 67.09 (t, NCH_2CH_2OH); 68.23 (s, $OOCCH(CH_3)OH$); 182.36 (s, $OOCCH(CH_3)OH$).

Preparation of Free Standing Iongel Materials: The cholinium-based iongel materials were prepared using a procedure previously developed for the preparation of imidazolium-based iongels by supramolecular PVA/phenol interactions.[31] In a typical experiment to prepare the PVA-TA-[Ch][Lac] iongel with 10 wt% of polymer concentration, 0.05 g of PVA was dissolved at 90°C in 0.5 g of water under vigorous stirring. Then, 0.5 g of [Ch][Lac] IL was added, followed by 0,034 g of TA. After complete dissolution of all the components, the mixed solution was poured into silicone molds and left at room temperature until gelation.

Characterization Methods: ATR-FTIR spectra were collected using a Bruker ALPHA spectrometer from 400 to 4000 cm^{-1}. The resolution was 4 cm^{-1} after 24 scans and the samples were placed directly on the ATR crystal. Thermogravimetric analyses (TGA) were carried out on a TGA Q500 device from TA instruments. The samples (≈10 mg) were heated at a constant rate of 10 °C min^{-1}, from 25 to 250 °C, under nitrogen atmosphere. The temperature at maximal decomposition rate (T_{max}) was determined as the temperature at main peak of the derivative weight loss curve. The measurements to assess the rheological behavior of the cholinium-based iongels were performed in an Anton Paar Physica MCR 301 rheometer. The gel–sol transition temperatures ($T_{gel\text{-}sol}$) were investigated by dynamic mechanical thermal analysis (DMTA) using a parallel-plate geometry (8 mm in diameter). The whole temperature studied ranged from 20 to 120°C with a heating rate of 2 °C min^{-1}. The experiments were conducted at a frequency of 1.0 Hz and 0.1% of strain. In order to study the elastic behavior of the iongels, compression tests were carried out in a universal testing machine (INSTRON 3344) at 23 °C and 55% of relative humidity. Iongel samples were prepared with roughly 1 mm of thickness and then subjected to compression tests, in which a 10 mm diameter plane-tip was moved down at a constant speed (1 mm min^{-1}), until the compressing samples achieved 40% of

their height. Pressure tests were performed in a mechanical testing machine, TA HD Plus Texture Analizer, by varying the pressure applied with a rate of 0.6 mm min^{-1}. Capacitance values were measure with a Multimeter LOMVUN T28B.

Ionic Conductivity Measurements: The ionic conductivity was measured by electrochemical impedance spectroscopy (EIS) using a Autolab 302N potentiostat galvanostat coupled to a Microcell HC station to control the temperature during the measurements. Circular iongels were used for the measurements (diameter = 8 mm). The iongels were sandwiched between two electrodes made of stainless steel and sealed in a Microcell. The measurements were carried out from 20 to 60 °C with a step of 10°C holding the temperature for 20 min before each temperature to allow temperature equilibration. The frequency range was set from 1.10^{-5} to 1 Hz, and the amplitude was 10 mV.

3D Printing by Material Extrusion: The printing process was carried out in a 3D-Bioplotter (Developer Series, Envision TEC, Gladbeck, Germany) and the printing geometries were originally designed in Autodesk Inventor 2019. Typically, the printing of the samples was performed at a temperature of 120°C, with 0.001 mm of maximum resolution, and a maximum pressure of 1×10^5 Pascal. Needles with an inner diameter of 0.3 and 0.4 mm were used in this work.

Pressure Sensor Fabrication: Two separated iongel layers with 2 mm of thickness and 4,24 cm^2 of area were produced by 3D printing using the previously described extrusion conditions. The 3D printing process was design to get a copper wire inset into the iongel layer, as it could be visualized in the Video S 1 in the Supporting Information. Then, the pressure sensor was constructed by assembling both iongel layers in a sandwich type structure insulated with a plastic film with a thickness of around 20 µm (plastic wrap).

Fabrication of PEDOT:PSS Electrodes on Kapton Foil: These electrodes were fabricated following the procedure published elsewhere.[8] A kapton foil was covered with Cr 5 and 150 nm of gold by electrodeposition (BOC Edwards).The coated kapton foil was then laser cut (LPKF protolaser S) with the desired electrode shape (1 cm^2 round electrode and 2 cm by 3 mm connection). The PEDOT:PSS/DVS solution, prepared by following a previously reporter procedure,[53] solution was drop-casted and dried at 50 °C for 1 h. Then, each of the supramolecular cholinium-based iongels employed, namely PVA-TA-[Ch][Lac] and PVA-PGA-[Ch][Lac], were deposited.

Characteristics of Medical Electrodes Used: Gima 33371 universal electrodes for ECG, diameter 48 × 50 mm. Kapton electrodes 300HN from Dupont with 75 µm of thickness were used.

Fabrication of Textile Electrodes: The bracelet electrodes were fabricated following a previously reported method.[53,54] Briefly, polydimethylsiloxane (PDMS) was selectively deposited on a polyester stripe and thermally annealed to create a 1 cm^2 area surrounded by waterproof borders. Then a PEDOT:PSS/DVS solution was deposited by drop-casting technique. The PEDOT:PSS/DVS mixture was made using 10 mL of PEDOT:PSS (Clevios PH1000) from Heraeous, 5% v/v Ethylene Glycol from Sigma, 50 µL of 4-dodecylbenzenesulfonic acid (DBSA) from Sigma and 1% v/v DVS from Sigma and mixed by mechanical stirring. Thanks to the PDMS, the PEDOT solution remained on the desired area and was annealed at 50 °C for 1 h. Then, the PVA-TA-[Ch][Lac] iongel was heated up and deposited on top. Once the iongel cools down, the electrode was ready for recording.

ECG Acquisition and Signal Processing: *The* ECGs were recorded using a Sienna Ultimate device plugging the two electrodes to compare to ECG entries. The RE used was always a fresh medical electrode located on the left bottom of the chest. WE and CE were located on the wrists. The signal was then recorded with a hardware notch filter at 50 Hz. Before plotting the different ECGs, the signal was processed using an infinite impulse response (IIR) notch filter at 50, 100, and 150 Hz.

Supporting Information

Supporting Information is available from the Wiley Online Library or from the author.

Acknowledgements

This work was supported by Marie Sklodowska-Curie Research and Innovation Staff Exchanges (RISE) under the grant agreement No 823989 "IONBIKE". The financial support received from CONICET, UNL, and ANPCyT (Argentina) is also gratefully acknowledged. L.C.T. has received funding from the European Union's Horizon 2020 research and innovation programme under the Marie Sklodowska-Curie grant agreement no. 745734 and from FCT (Fundação para a Ciência e a Tecnologia) in Portugal under the research contract CEECIND/01697/2018.

Conflict of Interest

The authors declare no conflict of interest.

Data Availability Statement

The data that support the findings of this study are available from the corresponding author upon reasonable request.

Keywords

3D printing, supramolecular iongels, bioelectronics, body sensors, cholinium carboxylate ionic liquids

Received: February 23, 2021
Revised: April 21, 2021
Published online: June 17, 2021

[1] M. Amjadi, K. U. Kyung, I. Park, M. Sitti, *Adv. Funct. Mater.* **2016**, *26*, 1678.
[2] J. He, Y. Zhang, R. Zhou, L. Meng, T. Chen, W. Mai, C. Pan, *J. Mater.* **2020**, *6*, 86.
[3] P. Leleux, C. Johnson, X. Strakosas, J. Rivnay, T. Hervé, R. M. Owens, G. G. Malliaras, *Adv. Healthcare Mater.* **2014**, *3*, 1377.
[4] N. Joshi, K. Rawat, P. R. Solanki, H. B. Bohidar, *Sens. Bio-Sensing Res.* **2015**, *5*, 105.
[5] A. F. De Anastro, L. Porcarelli, M. Hilder, C. Berlanga, M. Galceran, P. Howlett, M. Forsyth, D. Mecerreyes, *ACS Appl. Energy Mater.* **2019**, *2*, 6960.
[6] L. C. Tomé, I. M. Marrucho, *Chem. Soc. Rev.* **2016**, *45*, 2785.
[7] A. Soroudi, N. Hernández, J. Wipenmyr, V. Nierstrasz, *J. Mater. Sci. Mater. Electron.* **2019**, *30*, 16666.
[8] M. Isik, T. Lonjaret, H. Sardon, R. Marcilla, T. Herve, G. G. Malliaras, E. Ismailova, D. Mecerreyes, *J. Mater. Chem. C* **2015**, *3*, 8942.
[9] E. Bihar, T. Roberts, E. Ismailova, M. Saadaoui, M. Isik, A. Sanchez-Sanchez, D. Mecerreyes, T. Hervé, J. B. De Graaf, G. G. Malliaras, *Adv. Mater. Technol.* **2017**, *2*, 1600251.
[10] J. Sun, Y. Yuan, G. Lu, L. Li, X. Zhu, J. Nie, *J. Mater. Chem. C* **2019**, *7*, 11244.
[11] H. Qin, R. E. Owyeung, S. R. Sonkusale, M. J. Panzer, *J. Mater. Chem. C* **2019**, *7*, 601.
[12] E. Sanchez-Rexach, T. G. Johnston, C. Jehanno, H. Sardon, A. Nelson, *Chem. Mater.* **2020**, *32*, 7105.
[13] A. M. Pekkanen, R. J. Mondschein, C. B. Williams, T. E. Long, *Biomacromolecules* **2017**, *18*, 2669.
[14] B. Narupai, A. Nelson, *ACS Macro Lett.* **2020**, *9*, 627.
[15] H. Nulwala, A. Mirjafari, X. Zhou, *Eur. Polym. J.* **2018**, *108*, 390.

[16] A. Kavanagh, R. Byrne, D. Diamond, K. J. Fraser, *Membranes (Basel)* **2012**, *2*, 16.
[17] S. Yamada, H. Toshiyoshi, *ACS Appl. Mater. Interfaces* **2020**, *12*, 36449.
[18] P. Wang, D. Pei, Z. Wang, M. Li, X. Ma, J. You, C. Li, *Chem. Eng. J.* **2020**, *398*, 125540.
[19] B. He, Y. Zhou, Z. Wang, Q. Wang, R. Shen, S. Wu, *Sens. Actuators, A* **2018**, *272*, 341.
[20] H. Wang, Z. Wang, J. Yang, C. Xu, Q. Zhang, Z. Peng, *Macromol. Rapid Commun.* **2018**, *39*, 1800635.
[21] Y. Ren, J. Guo, Z. Liu, Z. Sun, Y. Wu, L. Liu, F-. Yan, *Sci. Adv.* **2019**, *5*, eaax0648.
[22] D. M. Correia, L. C. Fernandes, P. M. Martins, C. García-Astrain, C. M. Costa, J. Reguera, S. Lanceros-Méndez, *Adv. Funct. Mater.* **2020**, *30*, 1909736.
[23] J. Cui, Y. Li, D. Chen, T. G. Zhan, K. D.a Zhang, *Adv. Funct. Mater.* **2020**, *30*, 2005522.
[24] C. W. Lai, S. S. Yu, *ACS Appl. Mater. Interfaces* **2020**, *12*, 34235.
[25] J. Wong, A. Basu, M. Wende, N. Boechler, A. Nelson, *ACS Appl. Polym. Mater.* **2020**, *2*, 2504
[26] L. Zhang, A. S. Ravipati, S. R. Koyyalamudi, S. C. Jeong, N. Reddy, P. T. Smith, J. Bartlett, K. Shanmugam, G. Münch, M. J. Wu, *J. Agric. Food Chem.* **2011**, *59*, 12361.
[27] N. Sahiner, S. Sagbas, M. Sahiner, C. Silan, N. Aktas, M. Turk, *Int. J. Biol. Macromol.* **2016**, *82*, 150.
[28] M. Petkovic, J. L. Ferguson, H. Q. N. Gunaratne, R. Ferreira, M. C. Leitão, K. R. Seddon, L. P. N. Rebelo, C. S. Pereira, *Green Chem.* **2010**, *12*, 643.
[29] P. Niamlang, T. Tongrain, P. Ekabutr, P. Chuysinuan, P. Supaphol, *J. Drug Delivery Sci. Technol.* **2017**, *38*, 36.
[30] E. M. Euti, A. Wolfel, M. L. Picchio, M. R. Romero, M. Martinelli, R. J. Minari, C. I. A. Igarzabal, *Macromol. Rapid Commun.* **2019**, *40*, 1900217.
[31] G. C. Luque, M. L. Picchio, A. P. S. Martins, A. Dominguez-Alfaro, L. C. Tomé, D. Mecerreyes, R. J. Minari, *Macromol. Biosci.* **2020**, *20*, 2000119.
[32] E. S. Morais, N. H. C. S. Silva, T. E. Sintra, S. A. O. Santos, B. M. Neves, I. F. Almeida, P. C. Costa, I. Correia-Sá, S. P. M. Ventura, A. J. D. Silvestre, M. G. Freire, C. S. R. Freire, *Carbohydr. Polym.* **2019**, *206*, 187.
[33] L. C. Tomé, D. Mecerreyes, *J. Phys. Chem. B* **2020**, *124*, 8465.
[34] A. Y. Yuen, L. Porcarelli, R. H. Aguirresarobe, A. Sanchez-Sanchez, I. del Agua, U. Ismailov, G. G. Malliaras, D. Mecerreyes, E. Ismailova, H. Sardon, *Polymers (Basel)* **2018**, *10*, 989.
[35] Y. Cao, Y. J. Tan, S. Li, W. W. Lee, H. Guo, Y. Cai, C. Wang, B. C. K. Tee, *Nat. Electron.* **2019**, *2*, 75.
[36] Y. J. Son, J. W. Bae, H. J. Lee, S. Bae, S. Baik, K. Y. Chun, C. S. Han, *J. Mater. Chem. A* **2020**, *8*, 6013.
[37] M. Serhan, M. Sprowls, D. Jackemeyer, M. Long, I. D. Perez, W. Maret, N. Tao, E. Forzani, *AIChE Annual Meeting Conf. Proc.*, American Institute of Chemical Engineers, New York **2019**.
[38] L. De Liao, I. J. Wang, S. F. Chen, J. Y. Chang, C. T. Lin, *Sensors* **2011**, *11*, 5819.
[39] S. B. Kesner, R. D. Howe, *IEEE/ASME Trans. Mechatronics* **2011**, *16*, 866.
[40] J. Y. Lee, J. An, C. K. Chua, *Appl. Mater. Today* **2017**, *7*, 120.
[41] M. L. Hammock, A. Chortos, B. C. K. Tee, J. B. H. Tok, Z. Bao, *Adv. Mater.* **2013**, *25*, 5997.
[42] S. Gong, Y. Wang, L. W. Yap, Y. Ling, Y. Zhao, D. Dong, Q. Shi, Y. Liu, H. Uddin, W. Cheng, *Nanoscale Horiz.* **2018**, *3*, 640.
[43] I. You, B. Kim, J. Park, K. Koh, S. Shin, S. Jung, U. Jeong, *Adv. Mater.* **2016**, *28*, 6359.
[44] T. Q. Trung, N. E. Lee, *Adv. Mater.* **2016**, *28*, 4338.
[45] D. D. Han, Y. L. Zhang, J. N. Ma, Y. Q. Liu, B. Han, H. B. Sun, *Adv. Mater.* **2016**, *28*, 8328.
[46] T. P. Huynh, P. Sonar, H. Haick, *Adv. Mater.* **2017**, *29*, 1604973.
[47] S. C. B. Mannsfeld, B. C. K. Tee, R. M. Stoltenberg, C. V. H. H. Chen, S. Barman, B. V. O. Muir, A. N. Sokolov, C. Reese, Z. Bao, *Nat. Mater.* **2010**, *9*, 859.
[48] Z. Lei, Q. Wang, S. Sun, W. Zhu, P. Wu, *Adv. Mater.* **2017**, *29*, 1700321.
[49] X. Pu, M. Liu, X. Chen, J. Sun, C. Du, Y. Zhang, J. Zhai, W. Hu, Z. L. Wang, *Sci. Adv.* **2017**, *3*, 1700015.
[50] D. Pani, A. Dessi, J. F. Saenz-Cogollo, G. Barabino, B. Fraboni, A. Bonfiglio, *IEEE Trans. Biomed. Eng.* **2016**, *63*, 540.
[51] E. Bihar, T. Roberts, E. Ismailova, M. Saadaoui, M. Isik, A. Sanchez-Sanchez, D. Mecerreyes, T. Hervé, J. B. De Graaf, G. G. Malliaras, *Adv. Mater. Technol.* **2017**, *2*, 1600251.
[52] L. C. Tomá, D. J. S. Patinha, R. Ferreira, H. Garcia, C. S. Pereira, C. S. R. Freire, L. P. N. Rebelo, I. M. Marrucho, *ChemSusChem* **2014**, *7*, 110.
[53] I. del Agua, D. Mantione, U. Ismailov, A. Sanchez-Sanchez, N. Aramburu, G. G. Malliaras, D. Mecerreyes, E. Ismailova, *Adv. Mater. Technol.* **2018**, *3*, 1700322.
[54] S. Takamatsu, T. Lonjaret, D. Crisp, J. M. Badier, G. G. Malliaras, E. Ismailova, *Sci. Rep.* **2015**, *5*, 15003.